Mixed Convective Transport Around Staggered Rows of Square Cylinders

Dipankar Chatterjee* and Bittagopal Mondal

Advanced Design and Analysis Group, CSIR - Central Mechanical Engineering Research Institute, Durgapur-713209, India

Abstract: The unsteady mixed convective transport around multiple bluff objects placed in a staggered configuration with respect to a uniform free stream flow is analyzed through two-dimensional numerical computation. The bluff objects are identical in shape and size with square cross-section and arranged in two different rows within an unconfined domain. A small temperature difference between the objects and the free stream results in the free convection in addition to the forced flow. Simulation is carried out using a finite volume based method considering a uniform cross flow of air (Prandtl number = 0.71) at a moderate Reynolds number (= 100). The transverse spacing between the cylinders may anticipated to influence significantly the wake dynamics, which in turn affects the thermal transport. Simultaneously, the mixed convective strength also influences the wake dynamics and vortex structure formation. An interplay between these two effects aptly dictates the resulting flow dynamics and associated thermal transport. Accordingly, the dimensionless transverse spacing is varied (= 1, 3 and 5) along with the mixed convective strength (Richardson number = 0-2). It is observed that the flow and thermal fields show chaotic nature at smaller transverse spacing. However, at larger spacing, the usual unsteady vortex dynamics persists. Very interestingly it is observed that the chaotic flow at smaller transverse spacing reduces its instability to become unsteady periodic at larger strength of the thermal buoyancy. The average heat transfer from the cylinders is found more at smaller transverse spacings and it increases with increasing mixed convective strength.

Keywords: Mixed convection, Square cylinder, Staggered arrangement, Vortex shedding, Unsteady periodic flow, Heat transfer.

1. INTRODUCTION

The unsteady thermo-fluidic transport around multiple bluff bodies is of practical engineering importance and has attracted a considerable amount of interest in the recent past. Such flows typically encounter in the offset-strip and louvered fin heat exchangers [1]. Other common applications are in the porous media, fluidized beds to name a few. As such, the fluid-dynamic interactions among multiple bodies fixed in an incident flow are a question common to biomechanics, multiphase flows and fluid-structure interactions. Furthermore, the study is of significant fundamental interest since the wake interactions among multiple bluff objects create a complex flow structure that result in a variety of unexpected flow phenomena. Examples are the wake unsteadiness and the onset of chaos even at small Reynolds numbers. The thermal transport is dictated by this complex flow structure. A thorough knowledge of the involved wake dynamics is required for better understanding of the thermal transport in the wakes which is essential for the development of many of the thermal equipments.

Studies on the thermo-fluidic transport around rows of circular cylinders are available in plenty and are performed in majority for a relatively larger Reynolds numbers. These are reviewed in [2, 3]. However, similar studies for square cylinders at low to moderate Reynolds numbers are infrequent [4-11]. Chatterjee *et al*. [12-14] through a series of recent articles demonstrated numerically the effect of cylinder spacing on vortex dynamics, forced and mixed convective transport around a row of five in-line square cylinders in an infinite medium. In a subsequent effort, they [15, 16] extended the studies for the staggered rows of square cylinders with an emphasis to the onset of chaotic flow and forced convective transport. The introduction of thermal buoyancy and particularly the cross buoyancy (when buoyancy and free stream flow interacts cross wise) may believed to play a role of paramount importance on the resulting wake dynamics. The wake structure changes significantly with change in the transverse spacing of the cylinders as well as with the change in the mixed convective strength. The objective of this study is to understand the interplay between these two effects on the evolved flow dynamics and thermal transport.

2. MATHEMATICAL FORMULATIONS AND NUMERICAL SOLUTION

The objective is to analyze the mixed convective transport around two rows of fixed square cylinders arranged in a staggered fashion (Figure **1**) with various transverse spacings. The cylinders are assumed to be

*Address correspondence to this author at the Advanced Design and Analysis Group, CSIR - Central Mechanical Engineering Research Institute, Durgapur-713209, India; Tel: +91-343-6510455; Email: d_chatterjee@cmeri.res.in

E-ISSN: 2409-5826/19

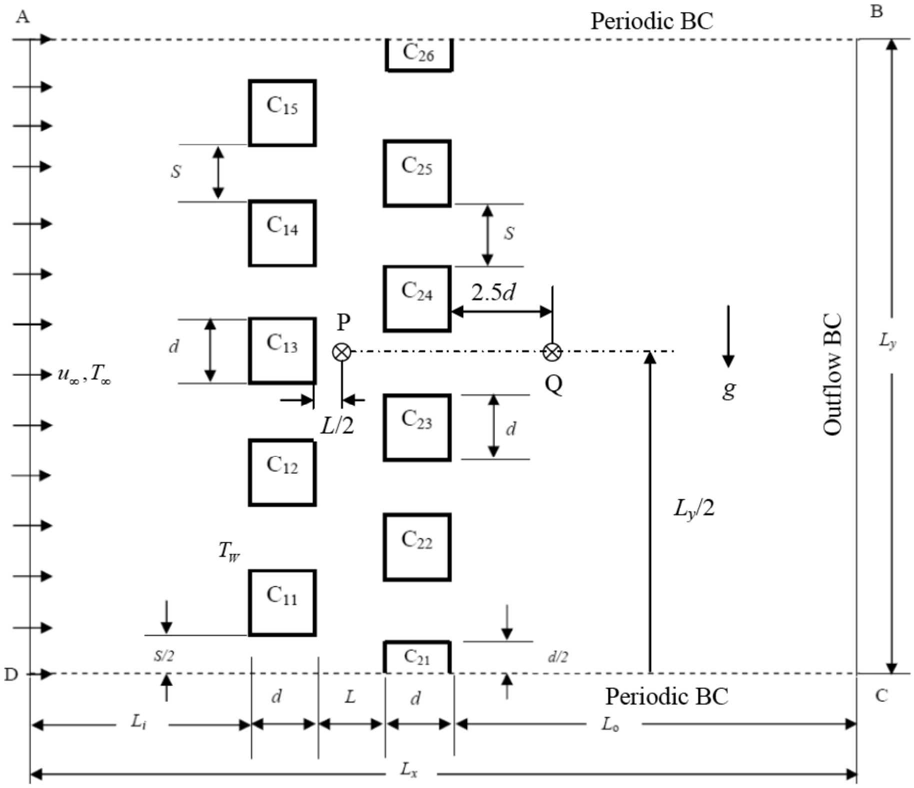

Figure 1: Schematic of the computational domain.

identical in shape and size (*d*) and exposed to a constant free stream with uniform velocity u_∞ and temperature T_∞. The cylinders are also heated to a constant temperature T_W ($> T_\infty$). The dimensionless transverse spacing between the cylinders is varied as *s/d* = 1, 3 and 5 where *S* is the transverse spacing. The Reynolds numbers is fixed to a moderate value (*Re* = 100) for a Richardson number (that governs the buoyancy-induced effect) range of $0 \le Ri \le 2$ with a fixed Prandtl number *Pr* = 0.71.

The dimensionless governing equations for the two-dimensional, unsteady, laminar, incompressible flow of Newtonian fluid with constant thermophysical properties along with Boussinesq approximation can be found in Ref. [14]. The pertinent dimensionless parameters are defined as: Reynolds number, *Re* ($= u_\infty d/\eta$), Richardson number, *Ri* ($= Gr/Re^2$), Grashof number, *Gr* ($= g\beta(T_W - T_\infty)d^3/\eta^2$) and Prandtl number, $Pr = \eta/\alpha$, with fluid properties, kinematic viscosity, η; volumetric expansion coefficient, β; thermal diffusivity, α with *g* being the acceleration due to gravity.

The following boundary conditions are invoked: at the inlet (face AD in Figure **1**), which is located $L_i = 7d$ upstream of the row of cylinders, a uniform flow with constant temperature is prescribed; at the outlet (face BC in Figure **1**), which is located at $L_0 = 30d$ downstream of the row of cylinders, an outflow boundary condition ($\partial\phi/\partial x = 0$ with ϕ denoting velocity/temperature) is given; a periodic boundary condition is prescribed on the lateral faces (AB and DC in Figure **1**) of the computational domain for extending the results to an infinite number of cylinders. The no-slip boundary condition along with prescribed temperature is imposed at the cylinder walls. The flow is assumed to start impulsively from rest.

The lift coefficient is computed from:

$$C_L = 2\int_S \left(-p\hat{n}_y + \tau_{xy}\hat{n}_x + \tau_{yy}\hat{n}_y\right) dS \tag{1}$$

where $\hat{n}_x$ and $\hat{n}_y$ are the components of the unit normal vector on the cylinder surface dS along *x* and *y* directions, respectively and the integrations are performed on the surface (*S*) of the cylinder, *p* is the dimensionless pressure. The dimensionless shear stress is given as:

$$\tau_{ij} = \frac{1}{Re}\left[\frac{\partial u_i}{\partial x_j} + \frac{\partial u_j}{\partial x_i}\right] \tag{2}$$

The Strouhal number, which characterizes the periodicity in a flow field, is defined as $\mathrm{St} = \mathrm{f\,d}/\mathrm{u}_\infty$ where f is the vortex shedding frequency. The local Nusselt number based on the cylinder dimension is calculated using the relation $Nu = hd/k$, where h is the local heat transfer coefficient and k is the thermal conductivity of the fluid. Surface average heat transfer at each face of the cylinder is obtained by integrating the local Nusselt number along the cylinder face. The time dependent total average cylinder Nusselt number is the total of the average Nusselt number at each face of the cylinder. The time average local Nusselt number is obtained by integrating the local Nusselt number over a large period of time.

The conservation equations subjected to the aforementioned boundary conditions are solved using a finite volume based CFD solver Ansys Fluent (version 14.0) [17]. The QUICK (Quadratic Upstream Interpolation Convective Kinetics) scheme is used for spatial discretization of the convective terms and a central difference scheme is used for the diffusive terms. PISO (Pressure-Implicit with Splitting of Operators) algorithm is used as the pressure-velocity coupling scheme. A suitable dimensionless time step size (0.008) is used in the computation satisfying the Courant-Friedrichs-Lewy (CFL) and the grid Fourier criteria. Finally, the algebraic equations are solved by using the Gauss-Siedel point-by-point iterative method in conjunction with the Algebraic Multigrid (AMG) method solver. The convergence criteria based on relative error for the inner (time step) iterations are set as 10^{-6} for the discretized equations.

The simulation domain is discretized by a non-uniform grid with a finer grid distribution near the cylinders to capture the viscous boundary layer as well as the wake and the vortex street behind the cylinders. In order to carry out the grid sensitivity study especially for the smaller transverse spacing ratio, computations are performed for *s/d* = 1 at *Ri* = 2 with three different grid sizes, *viz*., 470×124, 500×164 and 530×204 and the local Nusselt numbers are computed for some representative cylinders. The maximum percentage variation between the first two sets of grids is found to be within 2.38%, whereas the same for the last two sets of grids is within 0.62%. Hence 500×164 grid is chosen for *s/d* = 1. Similar studies are also performed for the other spacing ratios and final choices of grids are 500×348 and 500×388 for *s/d* = 3 and 5 respectively.

The numerical method was extensively verified with available computational and experimental results for the cross-flow around five in-line isothermal square cylinders in an infinite medium in some of our earlier works [12-14]. Hence it is not repeated here for the purpose of brevity. It is worthy to mention once again that there is no available numerical or experimental works for the configuration of obstacles considered in the present work.

3. RESULTS AND DISCUSSION

Simulations are performed for varying transverse spacing ratios as *s/d* = 1, 3 and 5 fixing the Reynolds number constant at *Re* = 100 and *Pr* = 0.71 with Richardson umber in the range $0 \le Ri \le 2$ in steps of 0.5. The fluid flow and heat transfer characteristics are found to be strongly dependent on the spacing ratio and the strength of buoyancy. The following subsections elucidate the role of these parameters on the overall thermo-fluid dynamics.

3.1. Flow Dynamics

The typical flow structure is presented in Figure **2** showing the instantaneous vorticity maps for different transverse spacings and Richardson numbers. The vorticity plots are presented at a dynamic steady state condition (50000 time iterations that corresponds to a dimensionless time instant of 400 using the dimensionless time step size of 0.008). From the instantaneous vorticity contours of *s/d* = 5 at *Ri* = 0 (*i.e.* with no buoyancy effect, pure forced flow), a synchronized shedding pattern can be observed. Some of the vortices are in-phase and some others are in anti-phase. These vortices are clearly visible and they remain distinct throughout the computational domain without any significant lateral spread. This is attributable to the relatively weak interactive flow pattern at a larger spacing of the cylinders. Similar kind of shedding pattern is also observed for the configuration *s/d* = 3 (not shown) at *Ri* = 0. However, as the *s/d* ratio is further decreased, for example at *s/d* = 1, the vortices do not remain distinct downstream of the computational domain, because of the strong wake interactions due to the smaller spacing between the cylinders. As the strength of buoyancy increases gradually ($Ri > 0$), the flow shows strong affinity to move up just downstream of the heated cylinders for all spacing ratios. It was observed in our earlier study for the case with a single row of square cylinders [14] that for relatively higher spacing ratios (*s/d* = 4, 3 and 2), the shedding process almost disappears at some critical value of *Ri* (critical Richardson number, Ri_{cr}), below which the vortices shed into the stream and the flow is characterized as unsteady periodic. This important observation marks the difference between the pure forced and mixed convection studies. For *s/d* = 4, 3 and 2 in the single row case [14], shedding was

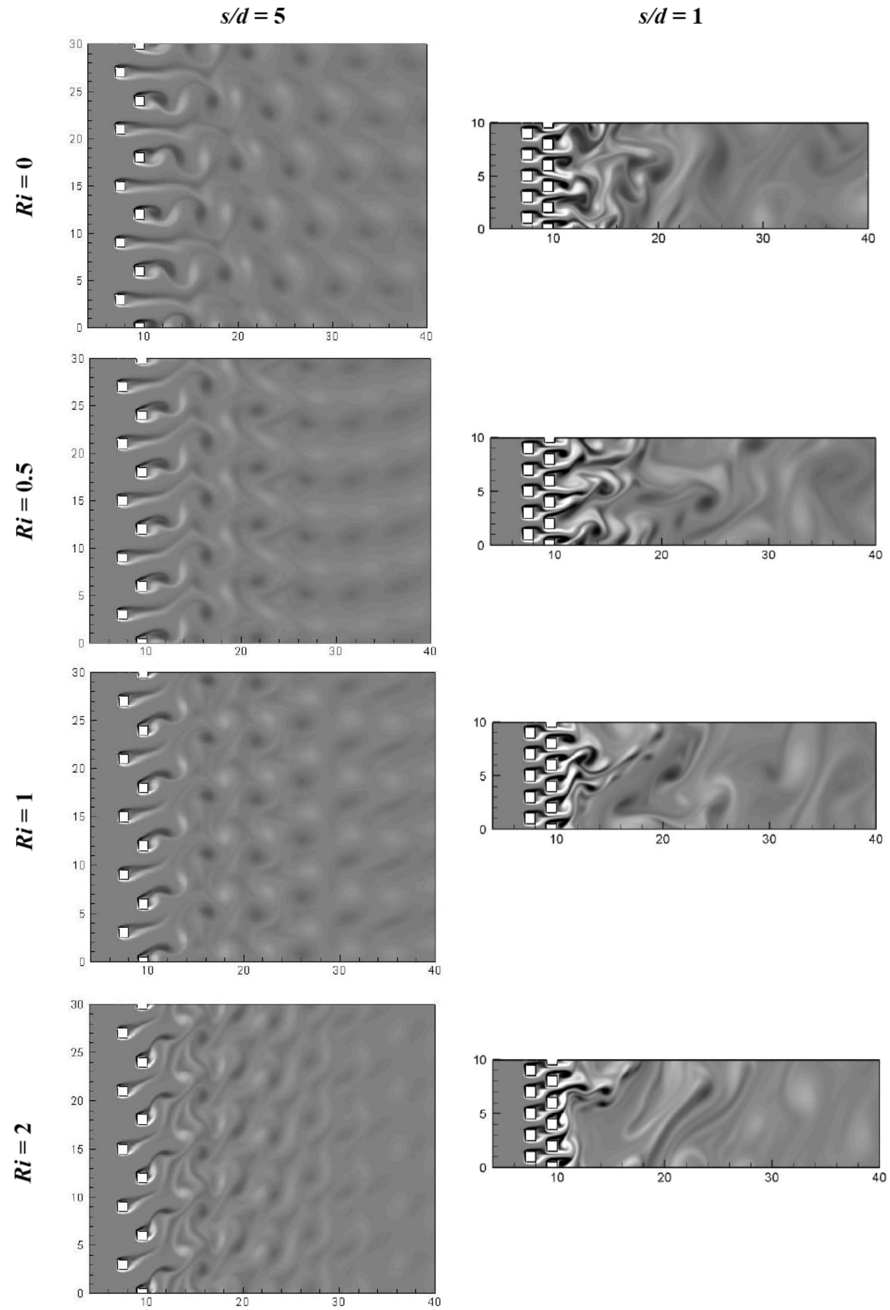

Figure 2: Vorticity contour plots for various *s/d* ratios and Richardson numbers.

observed to disappear at around $Ri_{cr} = 1.5$, 1.8 and 2.0, respectively. However, very interestingly, we observe here that such kind of flow features do not appear, *i.e.*, the flow is not observed to become steady by the increasing buoyancy effect. This suggests that the presence of the second row of the cylinders contributing significantly towards the flow instability. As such we increase the Richardson number up to 5 and still we get an unsteady periodic flow with occurrence of vortex shedding (not shown). Increasing Richardson number beyond that may put question on the applicability of the Boussinesq approximation.

With a reduction in the gap between the cylinders, more heating is required for the suppression of the flow instability. As the gap between the cylinders reduces, the gap velocity increases which destabilizes the flow and consequently more heating is required to stabilize it. At higher Richardson number, the fluid flows like buoyant plumes towards the upward direction. Furthermore, apart from the primary vortex shedding frequency, at smaller *s/d* ratio the wakes interact in a complicated manner to give rise to the secondary cylinder interaction frequencies that may induce additional instability to the flow. The secondary cylinder interaction frequency basically depends on the cylinder spacing. It is also related to transition between narrow and wide wakes behind a cylinder.

The above observations in regard to the hydrodynamics around staggered rows of square cylinder under mixed convection environment are quantitatively supported by looking into the lift coefficient signals and dimensionless frequency plots in Figures **3** and **4**, respectively. Figure **3** depicts the time response of the lift coefficient signals for representative cylinders (C13, C23 and C24) for various spacing ratios and Richardson numbers. At larger spacing ratio (*s/d* = 5) a sinusoidal response of the lift coefficient is visible. At lower *s/d* ratio (=1), as a result of the secondary cylinder interaction frequencies, the time response of lift coefficient does not show such kind of behavior. With increasing buoyancy effect, the amplitude of oscillation increases. Interestingly, it is observed that the flow instability is suppressed with increasing buoyancy effect for smaller spacing ratio. As a consequence of that the lift signal becomes sinusoidal in nature at larger *Ri* from the chaotic nature at smaller *Ri* for lower *s/d*. A power spectrum density analysis of the lift coefficient signal is subsequently carried out to obtain the dominant (primary) frequency of vortex

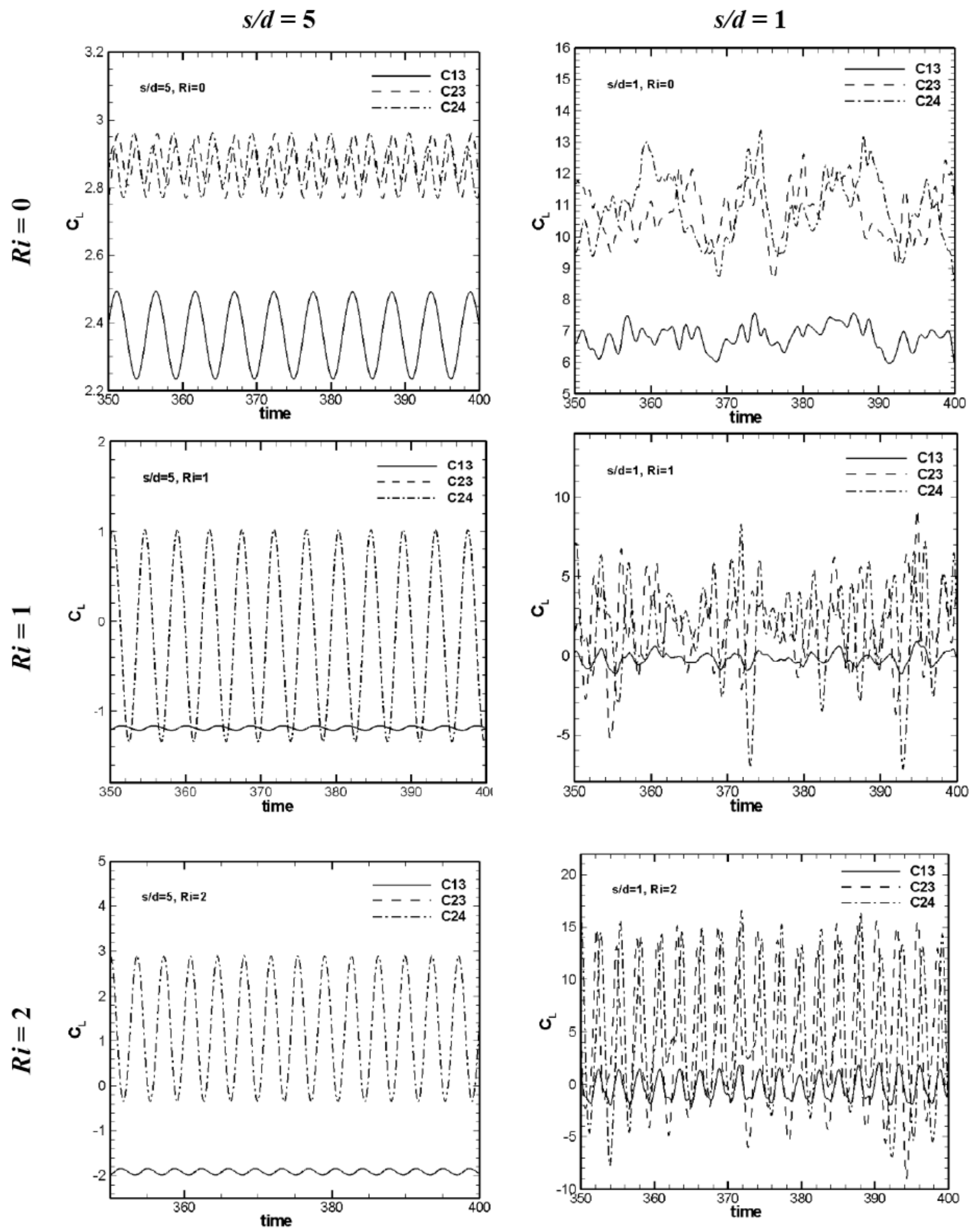

Figure 3: Time response of lift coefficient signals for representative cylinders for various *s/d* ratios and Richardson numbers.

shedding which is usually represented in terms of the Strouhal number (dimensionless frequency). Figure **4** shows the Strouhal number as function of the Richardson number for various transverse spacing. As we decrease the gap between the cylinders, the jet flow causes the frequency to increase substantially. This is also attributable to the existence of the secondary cylinder interaction frequency at smaller spacing. With increasing Richardson number, the Strouhal increases for moderate to larger spacing of the cylinders. This can be attributed by the fact that with increased heating, the fluid in the close proximity of the cylinders becomes hot and less dense and hence moves upwards. Consequently, the vortices do not remain attached to the cylinders for long periods. Since there is no vortex suppression, the Strouhal number is found to increase continuously with the Richardson number.

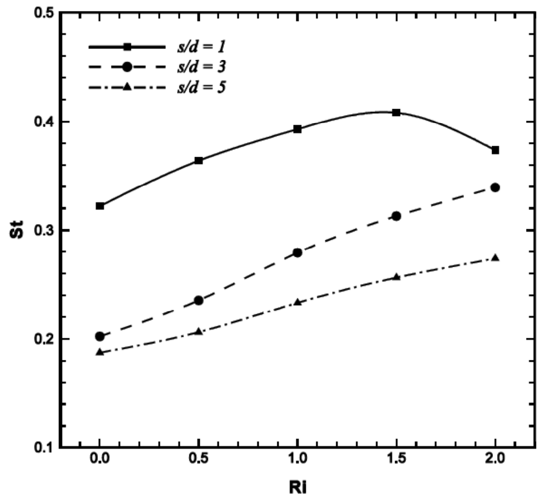

Figure 4: Strouhal number as function of Richardson number for various transverse spacing.

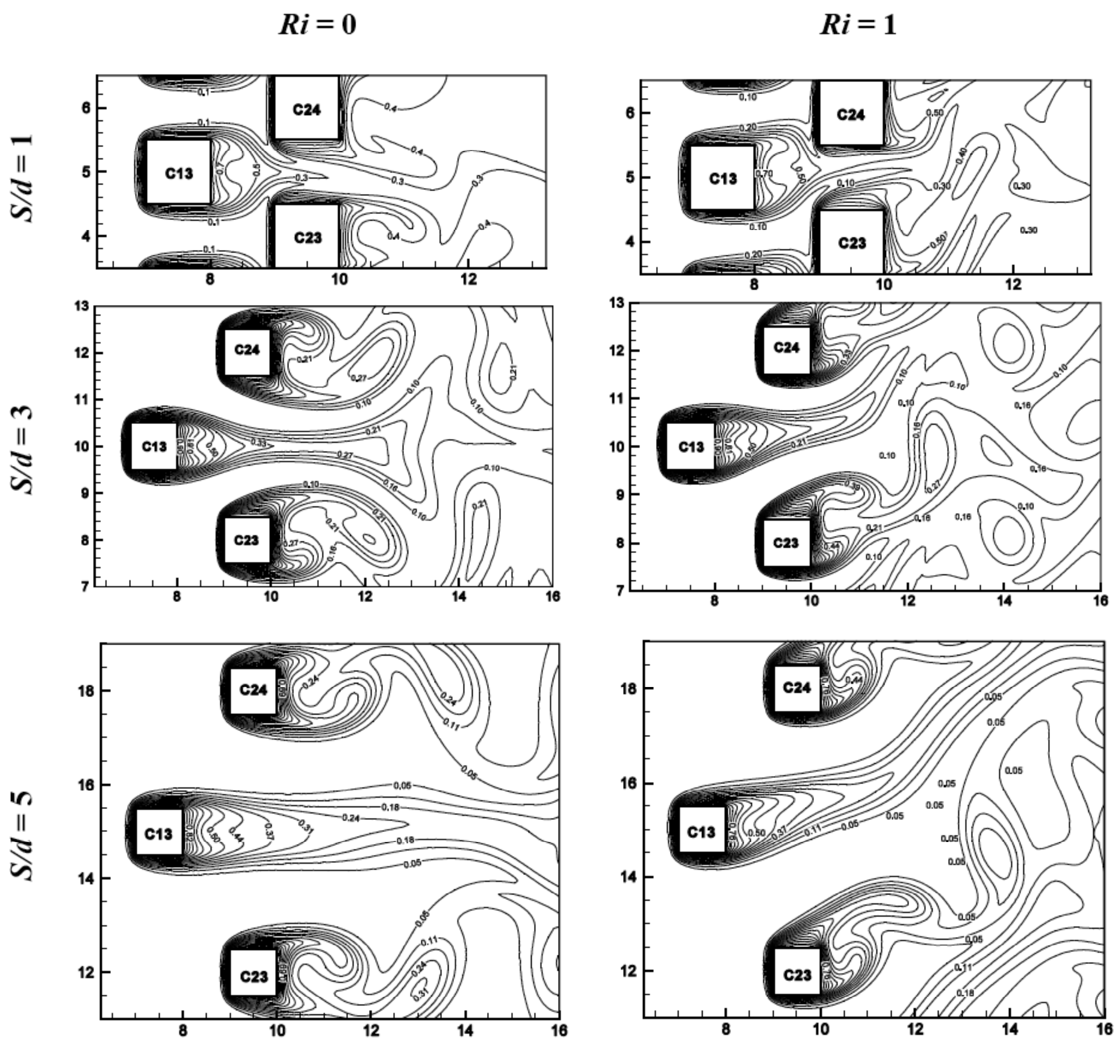

Figure 5: Isotherm profiles (closer views) for various *s/d* ratios and Richardson numbers.

3.2. Thermal Characteristics

Figure **5** shows the instantaneous isotherm contours (closer views around representative cylinders) at a dimensionless time = 400 for various *s/d* ratios and Richardson numbers. Since both the vorticity and thermal energy are transported by the flow itself, the vorticity contours as well as the isotherms exhibit similar features. The crowding of isotherms are precisely more on the frontal faces of the cylinders compared to the top, bottom and rear faces indicating a higher heat transfer rate at the front face. However, this organized nature of thermal transport is severely disrupted at smaller transverse spacing of the cylinders. A chaotic flow field significantly affects the heat transfer at this spacing and the resulting thermal fields become chaotic. The buoyancy causes the flow to become a plume like structure which is observed when the Richardson number increases.

In order to understand the effect of transverse spacing on the thermal transport, the average cylinder Nusselt numbers are computed for various spacing and plotted in Figure **6**. The average cylinder Nusselt number is computed by averaging the time and surface average Nusselt numbers of all the cylinders. It is interesting to observe that the average cylinder Nusselt number is more for smaller spacing. This suggests that the heat transfer increases at smaller spacing of the cylinders. This is justified since at smaller transverse spacing the flow becomes chaotic in nature resulting in enhanced mixing. This enhanced mixing eventually results in improved surface heat transfer coefficient causing an overall increase in the heat transfer rate. The increase of Nusselt number with Richardson number is obvious.

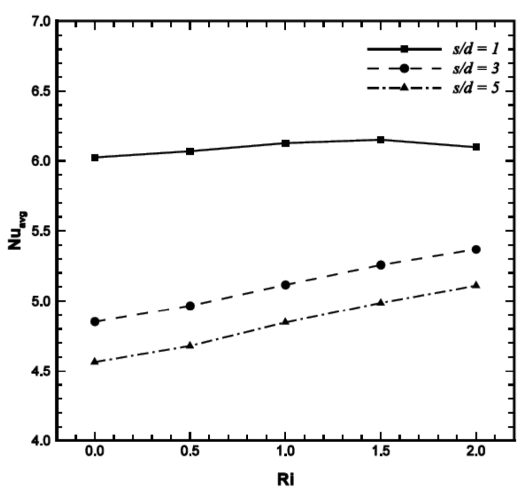

Figure 6: Time and surface average cylinder Nusselt number as function of Richardson number for various transverse spacing.

The distribution of the time average local Nusselt number for two adjacent cylinders placed side-by-side for *s/d* = 5 and different Richardson numbers is shown in Figure **7**. The front and rear surfaces are always showing highest and lowest Nusselt numbers, respectively for all cases signifying higher and lower heat transfer from those surfaces. At smaller transverse spacing the heat transfer is found more in comparison to larger transverse spacing because of the chaotic nature of the transport at smaller spacing as described earlier.

CONCLUSION

A two-dimensional numerical simulation is performed to analyze the mixed convective transport around two rows of staggered square cylinders placed in an unconfined domain. By fixing the Reynolds (*Re* =100) and Prandtl (*Pr* = 0.71) numbers, the influence of transverse cylinder spacing (*s/d*) on the coupled fluid flow and heat transfer is portrayed for a range of mixed convective strength (*Ri* = 0-2). The simulation confirms the existence of a chaotic flow regime for smaller transverse spacing under pure forced convective transport. However, with increasing buoyancy effect, the flow characteristics changes to a periodic state from the chaotic state thereby stabilizing the flow to some extent at smaller transverse gap. On the contrary, at the larger spacing of the cylinders, the flow is always of periodic nature and the stabilizing effect of the superimposed thermal buoyancy cannot be seen at least for the range of Richardson number considered because of the existence of the second row of the cylinders. The second row of the cylinders causes the secondary cylinder interaction frequency to evolve which makes the flow destabilized at larger spacing.

The other quantitative observations are as follows:

- The Strouhal frequency is observed to be more for smaller transverse spacing and it increases with increasing thermal buoyancy. However, at smaller spacing and larger buoyancy it further decreases;

- The average heat transfer rate from the cylinders is more for smaller spacing and the heat transfer increases with increasing Richardson number;

- More heat transfer rates are always predicted at the frontal faces of the cylinders in comparison to other surfaces.

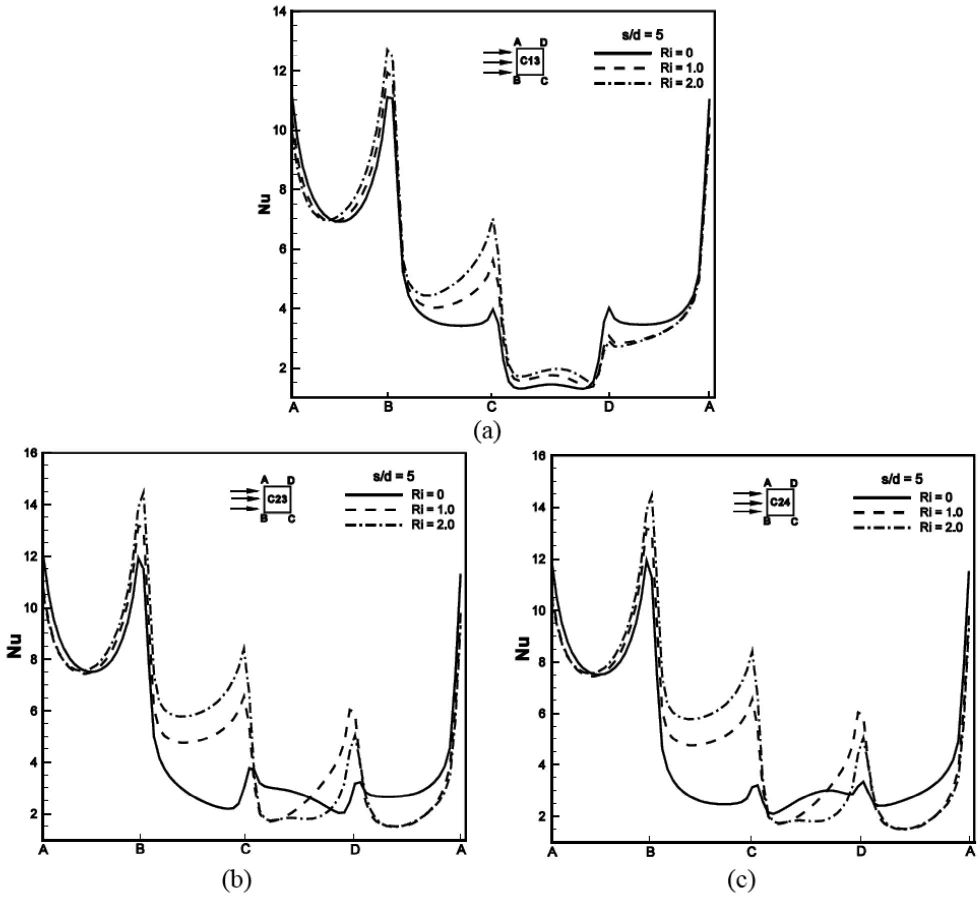

Figure 7: Distribution of time average local Nusselt number for two adjacent cylinders placed side-by-side for *s/d* = 5 and different Richardson numbers (**a**) C13 (**b**) C23 and (**c**) C24.

REFERENCES

[1] Sheui TWH, Tsai SF, and Chiang TP. Numerical study of heat transfer in two-row heat exchangers having extended fin surfaces. Numerical Heat Transfer A, 1999; 35: 797-814. https://doi.org/10.1080/104077899275038

[2] Zdravkovich MM. Flow around circular cylinders: Fundamentals, Oxford University Press, New York 1997.

[3] Zdravkovich MM. Flow around circular cylinders: Applications, Oxford University Press, New York 2003.

[4] Kumar SR, Sharma A, Agrawal A. Simulation of flow around a row of square cylinders. Journal of Fluid Mechanics, 2008; 606: 369-397. https://doi.org/10.1017/S0022112008001924

Sewatkar CM, Sharma A, Agrawal A. On the effect of Reynolds number for flow around a row of square cylinders. Physics of Fluids, 2009; 21: 083602 (1-13).

[5] Sewatkar CM, Patel R, Sharma A, Agrawal A. Flow around six in-line square cylinders. Journal of Fluid Mechanics, 2012; 710: 195-233. https://doi.org/10.1017/jfm.2012.359

[6] Sanyal A, Dhiman A. Effect of thermal buoyancy on a fluid flowing past a pair of side–by–side square bluff–bodies in a low–Reynolds number flow regime. Physics of Fluids, 2018; 30: 063603. https://doi.org/10.1063/1.5025652

[7] Sanyal A, Dhiman A. Wake interactions in a fluid flow past a pair of side-by-side square cylinders in presence of mixed convection. Physics of Fluids, 2017; 29: 103602. https://doi.org/10.1063/1.5005118

[8] Sarkar S, Dalal A, Biswas G. Mixed convective heat transfer from two identical square cylinders in cross flow at Re = 100. International Journal of Heat and Mass Transfer, 2010; 53: 2628-2642. https://doi.org/10.1016/j.ijheatmasstransfer.2010.02.053

[9] Patel CG, Sarkar S, Saha SK. Mixed convective vertically upward flow past side-by-side square cylinders at incidence. International Journal of Heat and Mass Transfer. 2018; 127: 927-947. https://doi.org/10.1016/j.ijheatmasstransfer.2018.06.129

Chatterjee D, Das SP. Transient mixed convection heat transfer around three isothermal square cylinders in cross-flow at low Reynolds numbers, Journal of Energy Heat and Mass Transfer (In Press).

[10] Chatterjee D, Biswas G, Amiroudine S. Numerical investigation of forced convection heat transfer in unsteady flow past a row of square cylinders. International Journal of Heat and Fluid Flow, 2009; 30: 1114-1128l. https://doi.org/10.1016/j.ijheatfluidflow.2009.09.004

[11] Chatterjee D, Biswas G, Amiroudine S. Numerical simulation of flow past row of square cylinders for various separation ratios. Computers and Fluids, 2010; 39: 49-59. https://doi.org/10.1016/j.compfluid.2009.07.002

[12] Chatterjee D, Biswas G, Amiroudine S. Mixed convection heat transfer from an in-line row of square cylinders in cross-flow at low Reynolds number. Numerical Heat Transfer A, 2012; 61: 891-911.

[13] Chatterjee D, Biswas G. Dynamic behavior of flow around rows of square cylinders kept in staggered arrangement, Journal of Wind Engineering and Industrial Aerodynamics,

2015; 136: 1-11. https://doi.org/10.1016/j.jweia.2014.10.019

[14] Chatterjee D, Gupta SK. Convective transport around rows of square cylinders arranged in a staggered fashion at moderate Reynolds number, Numerical Heat Transfer A, 2015; 68: 388-410. https://doi.org/10.1080/10407782.2014.986004

[15] ANSYS Fluent 14.0. (2009). Theory Guide, ANSYS Inc.

Received on 31-10-2018 Accepted on 2-1-2019 Published on 1-4-2019

DOI: http://dx.doi.org/10.15377/2409-5826.2019.06.2